

# Computational Fluid Dynamics study of Heat transfer enhancement in a circular tube using nanofluid

Abdolbaqi Mohammed Khdher.\*

Faculty of Mechanical Engineering, 26600, Pekan,  
Pahang, University Malaysia Pahang, Malaysia  
E-mail address: [abdolbaqi.mk@gmail.com](mailto:abdolbaqi.mk@gmail.com)

Wan Azmi Wan Hamzah, Rizalman Mamat  
Faculty of Mechanical Engineering, 26600, Pekan,  
Pahang, University Malaysia Pahang, Malaysia

**Abstract**—A study of computational fluid dynamics has been conducted to study the characteristics of the heat transfer and friction factor of CuO/water & Al<sub>2</sub>O<sub>3</sub>/water nanofluid flowing inside straight tube. The three dimensional realizable *k-ε* turbulent model with enhanced wall treatment was utilized. As well as were used Temperature dependent thermophysical properties of nanofluid and water. The evaluation of the overall performance of the tested tube was predicated on the thermo-hydrodynamic performance index. The obtained results showed that the difference in behaviour depending on the parameter that has been selected to compare the nanofluid with the base fluid. In addition, the friction factor and the heat transfer coefficient increases with an increase of the nanoparticles volume concentration at the same Reynolds number. The penalty of pressure drop is negligible with an increase of the volume concentration of nanoparticles. Conventional correlations that have been used in turbulent flow regime to predict average heat transfer and friction factor are Gnielinski correlation and Pak & Cho correlation, for tubes are also valid for the tested nanofluids which consider that the nanofluids have a homogeneous fluid behave.

**Index Terms**— Nanofluid; Heat transfer; Straight circular tube; CFD; ANSYS FLUENT

## I. INTRODUCTION

Using heat transfer enhancement techniques, can improve thermal performance of a tubes. The heat transfer techniques can be classified in to three broad techniques: Passive techniques that do not need external power such as rough surfaces, swirl flow devices, treated surfaces, extended surfaces, displaced enhancement devices, surface tension device, coiled tube and additives such as nanoparticles: Active technique that need external power to enable the wanted flow modification for increasing heat transfer such as electrostatic fields, mechanical aids, jet impingement, suction, injection, surface vibration, and fluid vibration: Compound technique is the mix of two or more of the techniques that mentioned above at one time. There are many applications of heat transfer augmentation by using nanofluids to get the cooling challenge necessary such as the photonics, transportation, electronics, and energy supply industries [1-5]. Examined the effect of volume fraction and temperature on the TiO<sub>2</sub>/ water nanofluid viscosity. Results recorded and that have been analyzed within a temperature range of 25 to 70°C and volume fraction 0.1, 0.4, 0.7 and 1%. Viscosity of the nanofluid was experimentally measured by [6]. Utilizing a rheometer. It obtained as a function of the nanoparticles shear rate and mass fraction. A double tube coaxial heat exchanger heated by solar energy using Aluminum oxide nanofluid presented experimentally and numerically by [7]. Results showed that the heat transfer performance of nanofluid higher than base fluid. Water already used as a

base fluid and two non-similar materials titanium dioxide (TiO<sub>2</sub>) and single wall carbon nanohorn (SWCNH). Results showed empirical correlation equations of viscosity. Forced convection turbulent flow of nanofluid (Al<sub>2</sub>O<sub>3</sub> / water) with variable wall temperature inside an annular tube has been experimentally investigated by [8]. The results shown due to the nanoparticle presence in the fluid the heat transfer has been enhanced. Horizontal double-tube heat exchanger counter turbulent flow studied numerically by [9, 10]. Studied the effect of the SiO<sub>2</sub> nanofluid on the automotive cooling system. The study has been included both experimental and simulation by FLUENT software. The results showed that significant of the nanofluid in heat transfer enhancement and also, good agreement with other experimental data. The turbulent flow of nanofluids (TiO<sub>2</sub>, Al<sub>2</sub>O<sub>3</sub> and CuO) with different volume concentrations flowing through a duct under constant heat flux condition with two-dimensional model has been analysed numerically [11].

In the current study, the enhancement of heat transfer in the straight tube is carried out. The CFD analysis by ANSYS FLUENT software using the finite volume method is adopted. The heat flux, Reynolds numbers and the CuO volume concentration are (5000W/m<sup>2</sup>), (10<sup>4</sup>-10<sup>6</sup>) and (1-3%) respectively. The nanofluids (Al<sub>2</sub>O<sub>3</sub> and CuO) dispersed to water are utilized. Results were validated by comparison with experimental data in the literatures.

## II. THERMAL PROPERTIES

The thermal properties of nanofluid such as density ( $\rho_{nf}$ ), specific heat capacity ( $C_{nf}$ ), thermal conductivity ( $k_{nf}$ ) and viscosity ( $\mu_{nf}$ ) of nanofluid is obtained by the relation [12].

$$\rho_{nf} = \left(\frac{\phi}{100}\right)\rho_p + \left(1 - \frac{\phi}{100}\right)\rho_f \quad (1)$$

$$C_{nf} = \frac{\frac{\phi}{100}(\rho C)_p + \left(1 - \frac{\phi}{100}\right)(\rho C)_f}{\rho_{nf}} \quad (2)$$

$$k_s = \frac{k_{nf}}{k_f} = 0.8938 \left(1 + \frac{\phi}{100}\right)^{1.37} \left(1 + \frac{T_{nf}}{70}\right)^{0.2777} \left(1 + \frac{d_p}{150}\right)^{-0.0336} \left(\frac{\alpha_p}{\alpha_f}\right)^{0.01737} \quad (3)$$

$$\mu_r = \frac{\mu_{nf}}{\mu_f} = \left(1 + \frac{\phi}{100}\right)^{1.13} \left(1 + \frac{T_{nf}}{70}\right)^{-0.038} \left(1 + \frac{d_p}{170}\right)^{-0.061} \quad (4)$$

The assumption of a problem undertaken is that the nanofluid comports as a Newtonian fluid for concentration less than 4.0%. For conditions of dynamic similarity for flow of the two media, nanoparticles and base liquid water in tube, the ratio of friction coefficients can be written as follows:

$$f_r = \frac{f_{nf}}{f_f} = \left[ \frac{C2}{C3} \right] \frac{Re_f^m}{Re_{nf}^p} \quad (5)$$

For base fluid water [13].

$$f_f = \frac{0.316}{Re^{0.25}} \quad (6)$$

The system of governing criteria can be written as:

$$f_r = \frac{f_{nf}}{f_f} = F \left[ \frac{\rho_{nf}}{\rho_f}, \frac{\mu_{nf}}{\mu_f} \right] \quad (7)$$

Number of investigators derive the empirical correlation from experimental data. [14-18].

$$f_r = \frac{f_{nf}}{f_f} = 1.078 \left[ \left( \frac{\rho_{nf}}{\rho_f} \right)^{-0.514} \left( \frac{\mu_{nf}}{\mu_f} \right)^{-0.1248} \right] \quad (8)$$

Forced convection heat transfer coefficient under turbulent flow may be estimated by Dittus-Boelter correlation (Eq. (9)) for pure water in the range of Reynolds number  $10^4 < Re < 10^5$ .

$$Nu = \frac{h_f}{k_f} D = 0.023 Re^{0.8} Pr^{0.4} \quad (9)$$

The modified Dittus-Boelter (Eq. (10)) is applicable for both water and nanofluids with spherical shaped nanoparticles dispersed in water as [14].

$$Nu_{nf} = \frac{h_{nf}}{k_{nf}} D = 0.023 Re^{0.8} Pr_f^{0.4} (1 + Pr_{nf})^{-0.012} (1 + \phi)^{0.23} \quad (10)$$

Reynolds number depending on the diameter of the tube can be defined as:

$$Re = \frac{\rho_{nf} \times D \times u}{\mu_{nf}} \quad (11)$$

The properties of the solid particles are taken to be steady in the present operating temperature of 298 K to 320 K. Thus, the properties of nanofluids are temperature

#### A. Governing equations

The single phase approach adopted for nanofluid modelling according to the assumption of solid particles

#### B. Boundary conditions.

Volume concentration nanofluids (1, 2 and 3%) at 25°C base temperature used for nanofluid as input. while water used as the working fluid for comparison purposes. CFD studies were conducted with uniform inlet velocity profile and pressure outlet condition used at the tube outlet. For an initial guess of turbulent quantities ( $k$  and  $\epsilon$ ), the turbulent intensity ( $I$ ) was specified. Where the turbulent intensity for each case can be calculated based on the formula.

$$I = 0.16 \times Re^{-1/8} \quad (17)$$

The wall of tube assumed to be perfectly smooth with constant heat flux condition of 5000 W/m<sup>2</sup> specified on the tube wall. Reynolds number varied from  $1 \times 10^4$  to  $1 \times 10^6$  at

dependent in simulations of this study. The nanofluids properties at the tube inlet section shows in table (1).

### III. COMPUTATIONAL METHOD

#### A. Physical model.

Cartesian geometry coordinates of problem undertaken showed in Fig. (1). The assumption of this study limited to be steady state, Newtonian and incompressible turbulent fluid flow, no effect of gravity, constant thermophysical properties of nanofluid, heat conduction in the axial direction and the tube wall thickness was neglected.

High Reynolds number as input parameter estimated; pressure treatment adopted High Reynolds number as input parameter estimated; pressure treatment adopted with 3D realizable k- $\epsilon$  turbulent model with enhanced wall treatment employed, for all the governing equations the converged solutions considered for residuals lower than 25000. The simulation results for nanofluid were compared with the equations of Blasius (Eq. (12)) for friction factor and Dittus-Boelter equation (Eq. (13)) for  $Nu$  as:

$$f = \frac{0.316}{Re^{0.25}} \quad (12)$$

$$Nu = \frac{h_f}{k_f} D_{eff} = 0.023 Re^{0.8} Pr^{0.4} \quad (13)$$

(10)

$$\frac{\partial \bar{u}}{\partial x} + \frac{\partial \bar{v}}{\partial y} + \frac{\partial \bar{w}}{\partial z} = 0 \quad (14)$$

$$\rho \left( \bar{u} \frac{\partial \bar{u}}{\partial x} + \bar{v} \frac{\partial \bar{u}}{\partial y} + \bar{w} \frac{\partial \bar{u}}{\partial z} \right) = -\frac{\partial \bar{p}}{\partial x} + \mu \nabla^2 \bar{u} - \frac{\partial}{\partial x} \rho \bar{u} \bar{u} - \frac{\partial}{\partial y} \rho \bar{u} \bar{v} - \frac{\partial}{\partial z} \rho \bar{u} \bar{w} \quad (15)$$

$$\rho \left( \bar{u} \frac{\partial \bar{v}}{\partial x} + \bar{v} \frac{\partial \bar{v}}{\partial y} + \bar{w} \frac{\partial \bar{v}}{\partial z} \right) = -\frac{\partial \bar{p}}{\partial y} + \mu \nabla^2 \bar{v} - \frac{\partial}{\partial x} \rho \bar{u} \bar{v} - \frac{\partial}{\partial y} \rho \bar{v} \bar{v} - \frac{\partial}{\partial z} \rho \bar{v} \bar{w} \quad (15)$$

$$\rho \left( \bar{u} \frac{\partial \bar{w}}{\partial x} + \bar{v} \frac{\partial \bar{w}}{\partial y} + \bar{w} \frac{\partial \bar{w}}{\partial z} \right) = -\frac{\partial \bar{p}}{\partial z} + \mu \nabla^2 \bar{w} - \frac{\partial}{\partial x} \rho \bar{u} \bar{w} - \frac{\partial}{\partial y} \rho \bar{v} \bar{w} - \frac{\partial}{\partial z} \rho \bar{w} \bar{w} \quad (16)$$

$$\rho c_p \left( \bar{u} \frac{\partial \bar{t}}{\partial x} + \bar{v} \frac{\partial \bar{t}}{\partial y} + \bar{w} \frac{\partial \bar{t}}{\partial z} \right) = k \nabla^2 \bar{t} - \frac{\partial}{\partial x} \rho c_p \bar{u} \bar{t} - \frac{\partial}{\partial y} \rho c_p \bar{v} \bar{t} - \frac{\partial}{\partial z} \rho c_p \bar{w} \bar{t} \quad (16)$$

(less than 100 nm). The dimensional conservation equations for steady state mean conditions for all these assumptions, are as follows: continuity, momentum and energy equations [19].

each step of iterations as input data. The friction factor and  $Nu$  introduced as output data.

#### C. Grid independence test.

Grids independence in Ansys software for tube as (20x100) cells and subdivisions in the axial length, and surface face, respectively tested. To find the most suitable size of mesh faces, grid independent test has been performed for the physical model. In the current study, triangular cells used to mesh the wall and surfaces of the tube. The grid independence verified by using different grid systems and three meshes face of (20x100, 40x100 and 20x200) for pure water. Nusselt number estimated for all four mesh faces and results were proper. Nevertheless, in this study, mesh faces with (20x100) has been adopted to be the best in terms of accuracy.

#### A. CFD simulation.

CFD simulations used *ANSYS* software with solver strategy and analyse problems. To make numerical solution possible for governing equations, used control volume approach to solve the single phase conservation equations then converting them to algebraic equations. Simulation results tested by comparing the predicted results [11, 20 & 21], that used circular heated tube in experimental work. CFD modelling region might be classified into few important steps: pre-process step, the problem geometry that undertaken has been constructed as flat narrow and the computational mesh was generated in Ansys 15. It pursued by the physical model, boundary conditions and supplementary parameters appropriate described in models setup and solving stage. All velocity constituents and all scalar values of the problem computed at the centre of control volume interfaces whereas the grid schemes intensively utilized. Throughout the iterative process accurately monitor of the residuals done. At the point when the residuals for all governing equations were less than  $10^{-6}$ , all solutions assumed to be converged. At last, the results could be acquired when the iterations of Ansys Fluent lead to converged solution defined by a set of converged criteria. The friction factor and Nusselt number inside the tube might be acquired all through the computational domain in the post-procedure stage. It can be seen in Fig. (2).

The grid independent test of the Nusselt number against Reynolds number with respect all of grid size mesh. It seems that all of the meshing size are proper but in this study, the mesh size (20x100) will be consider as an optimum meshing size

#### IV. RESULTS AND DISCUSSION

##### A. Verification process

The verification process is very important to check the results. It can be perceived in Fig. (3a), with an increase of Reynolds number the friction factor decreases under turbulent flow condition. The Blasius (Eq. (12)) results indicated as a solid black line. It appears that good agreement among the CFD results and the equations. On the other side, the results of the heat transfer coefficient show in Fig. (3b). The Dittus-Boelter (Eq. (13)) indicated also, as a solid black line. It seems that there is good agreement among the CFD analysis and the equation.

##### B. The effect of nanofluid type

Fig. (4a), shows the comparison of the friction factor CFD analysis results for ( $\text{Al}_2\text{O}_3$  and CuO) and pure water nanofluids at turbulent regime. It seems insignificant affect of the types of nanofluids on the friction factor under turbulent flow condition. Likewise, Fig. (4b), indicates the Nusselt number with Reynolds number of ( $\text{Al}_2\text{O}_3$  and CuO) and pure water nanofluids at turbulent regime. It can be perceived that highest values of Nusselt number detected at CuO nanofluid than others followed by  $\text{Al}_2\text{O}_3$ . The reason related to be highest values of Nusselt number for CuO may be the highest values of thermal conductivity and lowest viscosity.

Fig. (5), illustrates the local Nusselt number for CuO and  $\text{Al}_2\text{O}_3$  Nanofluid with volume fraction and nanoparticles diameter of 3% and 20nm respectively. The result

indicates that increasing Reynolds number cause to increase local Nusselt number. Due to the fact that higher Reynolds number provide higher velocity and temperature gradient at the tube.

##### C. The effect of nanofluid volume fraction

Heat transfer coefficient for CuO nanofluid and 1% to 3% volume fraction with Reynolds number demonstrates in Fig. (6). It seems that the nanofluid volume concentration effect is significant. As well as the heat transfer coefficient for pure water indicated also, as a solid line. The maximum deviation is 60% when the volume fraction increased from 1% to 3%.

##### D. Validation

Fig. (7), shows comparison among the equation that provided by Gnielinski and the calculated values of the Nusselt numbers for  $\text{Al}_2\text{O}_3$  nanofluid [19,20]. As observed, an excellent agreement has been obtained with calculated values from theoretical equation within a wide range of Reynolds numbers. It can be seen the Gnielinski and Pak and Cho correlations indicated as a dot black and solid black line respectively.

#### V. CONCLUSIONS

In the present study, Thermal properties of two types of nanoparticles suspended in water calculated depending on the equation of [19]. Forced convection heat transfer under turbulent flow by numerical simulation with uniform heat flux boundary condition of straight tube studied. The heat transfer enhancement due to various parameters such as Reynolds number and nanoparticle volume concentration reported. The governing equations has been solved using finite volume method with specific presumptions and proper boundary conditions. The Nusselt number and friction factor obtained through the numerical simulation. The study concluded that the enhancement of Nusselt number and friction factor are (25%) and (2%) for the narrow at all Reynolds numbers. The 3% volume concentration of nanofluid has the highest friction factor values, followed by (2 and 1%). The Nusselt number of CuO is the highest value followed  $\text{Al}_2\text{O}_3$ . There is a good agreement among the CFD analysis of Nusselt number and friction factor of nanofluid with experimental data of [11]. With deviation not more than 5%.

#### VI. ACKNOWLEDGEMENTS

The authors would like to be obliged to Universiti Malaysia Pahang for providing laboratory facilities.

#### REFERENCES

- [1]. Hussein A.M., Sharma K.V., Bakar R.A., Kadrigama K. (2014). Study of forced convection nanofluid heat transfer in the automotive cooling system. *Case Studies in Thermal Engineering*, 2, 50-61.
- [2]. Hussein A.M., Bakar R.A., Kadrigama K., & Sharma K.V. (2013). Experimental Measurements of Nanofluids Thermal Properties, *International Journal of Automotive & Mechanical Engineering*, 7, 850-864.
- [3]. Hussein A.M., Sharma K.V., Bakar R.A. & Kadrigama K. (2013). A review of forced convection heat transfer enhancement and hydrodynamic characteristics of a nanofluid. *Renewable and Sustainable Energy Reviews*, 29, 734-743.

- [4]. Meibodi M.E. (2010). An estimation for velocity and temperature profiles of nanofluids in fully developed turbulent flow conditions. *Int. Comm. in Heat and Mass Transfer*, 37,895-900.
- [5]. Bahiraei M., Hosseinalipour S.M., Zabihi K. & Taheran E. (2012). Using Neural Network for Determination of Viscosity in Water-TiO<sub>2</sub> Nanofluid. *Advances in Mechanical Engineering*, pp. 1687-8132.
- [6]. Bobbo S., Fedele L., Benetti A., Colla L., Fabrizio M., Pagura C. & Barison S. (2012). Viscosity of water based SWCNH and TiO<sub>2</sub> nanofluids. *Experimental Thermal and Fluid Science*, 36, 65-71.
- [7]. Luciu R.S., Mateescu T., Cotorobai V. & Mare T. (2009). Nusselt Number and Convection Heat Transfer Coefficient for a Coaxial Heat Exchanger Using Al<sub>2</sub>O<sub>3</sub>-water ph=5 nanofluid, *Bul. Inst. Polit. Ias, i, t. LV (LIX), f, 2*.
- [8]. Prajapati O.S. (2012). Effect of Al<sub>2</sub>O<sub>3</sub>-Water Nanofluids in Convective Heat Transfer. *Int. J. of Nano science*, 1, 1-4.
- [9]. Bozorgan N. & Mafi M. (2012). Performance Evaluation of Al<sub>2</sub>O<sub>3</sub>/Water Nanofluid as Coolant in a Double-Tube Heat Exchanger Flowing under a Turbulent Flow Regime, *Hindawi Publishing Corporation Advances in Mechanical Engineering*, 891382, 1-8.
- [10]. Hussein A.M., Bakar R.A., Kadirgama K. & Sharma K.V. (2013). The effect of nanofluid volume concentration on heat transfer and friction factor inside a horizontal tube. *Journal of Nanomaterials*, Article ID, 859563, 1-12.
- [11]. Rostamani, M, Hosseinizadeh. S.F, Gorji. M& Khodadadi. J.M. (2010). Numerical Study Of Turbulent Forced Convection Flow Of Nanofluids In A Long Horizontal Duct Considering Variable Properties. *International Communications in Heat and Mass Transfer*, 37, 1426-1431.
- [12]. Sharma, K. V., et al. "Correlations to predict friction and forced convection heat transfer coefficients of water based nanofluids for turbulent flow in a tube." *International Journal of Microscale and Nanoscale Thermal and Fluid Transport Phenomena* 3 (2010): 283-308.
- [13]. Sundar L.S.& Sharma K.V. (2010). Turbulent Heat Transfer and Friction Factor of Al<sub>2</sub>O<sub>3</sub> Nanofluid in Circular Tube with Twisted Tape Inserts, *Inter. J. Heat and Mass Transfer*, 53, 1409 – 1416.
- [14]. Dehghandokht M., Khan M.G., Fartaj A., Sanaye S. (2011). Flow and heat transfer characteristics of water and ethylene glycol-water in a multi-port serpentine meso-channel heat exchanger. *Int. J. of Thermal Sciences*.50, 1615-1627.
- [15]. Oliet C., Oliva A., Castro J., Segarra S.D. (2007). Parametric studies on automotive radiators. *Applied Thermal Engineering*, 27, 2033-2043.
- [16]. Leong K.Y., Saidur R., Kazi S.N.& Mamun A.M. (2010). Performance investigation of an automotive car radiator operated with nanofluid-based coolants (nanofluid as a coolant in a radiator). *Applied Thermal Engineering*, 30, 2685-2692.
- [17]. Gunnasegaran P., Shuaib N.H., Abdul Jalal M.F.& Sandhita E. (2012). Numerical Study of Fluid Dynamic and Heat Transfer in a Compact Heat Exchanger Using Nanofluids, *Int. Scholarly Res. Network ISRN Mechanical Engineering*, 2012,1-11.
- [18]. Durmus, M. Esen. (2002). Investigation of heat transfer and pressure drop in a concentric heat exchanger with snail entrance. *Applied Thermal Engineering*, 22, 321-332.
- [19]. Bejan A. (2004). *Convection Heat transfer*. New York: John Wiley & Sons Inc.
- [20]. Pak B.C. & Cho Y.I.(1998). Hydrodynamic and heat transfer study of dispersed fluids with submicron metallic oxide particles. *Exp. Heat Transfer*, 11, 70-151.
- [21]. Duangthongsuk W., Wongwises S. (2010). An Experimental Study on The Heat Transfer Performance and Pressure Drop of TiO<sub>2</sub>-water

nanofluids flowing under a Turbulent Flow Regime, *Int. J. of Heat and Mass Transfer*. 53,334-344.

## NOMENCLATURES

$C$	specific heat [W/kg.°C]
$D$	diameter [m]
$E$	energy [W]
$f$	friction factor
$h_{tc}$	convection heat transfer coefficient [W/m <sup>2</sup> .°C]
$k$	thermal conductivity [W/m.°C]
$Nu$	Nusselt number [ $h_{tc} .D/K_{nf}$ ]
$P$	pressure [N/m <sup>2</sup> ]
$Pr$	Prandtl number [ $C.\mu/K_{nf}$ ]
$Re$	Reynolds number [ $\rho_{nf}D_h u/K_{nf}$ ]
$u$	velocity [m/s]
$\mu$	viscosity [N.s/m <sup>2</sup> ]
$\rho$	density [kg/m <sup>3</sup> ]
$\tau$	shear stress [N/m <sup>2</sup> ]
$\phi$	volume concentration

## Subscripts

$f$	liquid phases
$p$	solid particle
$nf$	nanofluid

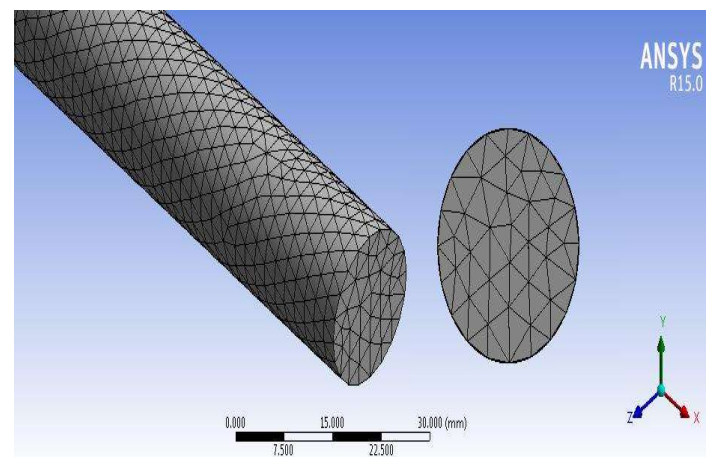


**Fig. 1. Geometrical model**

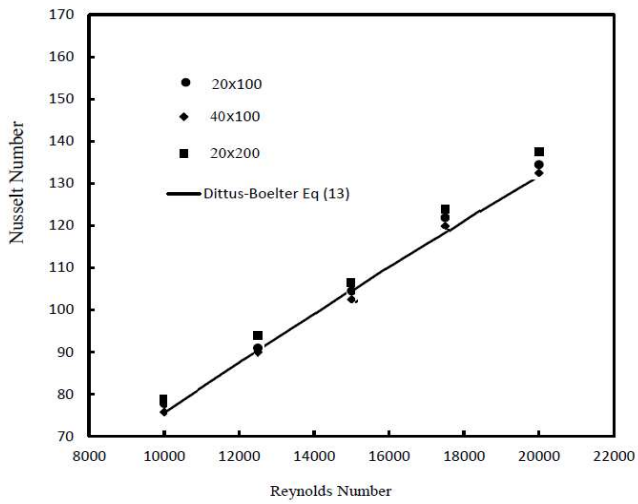
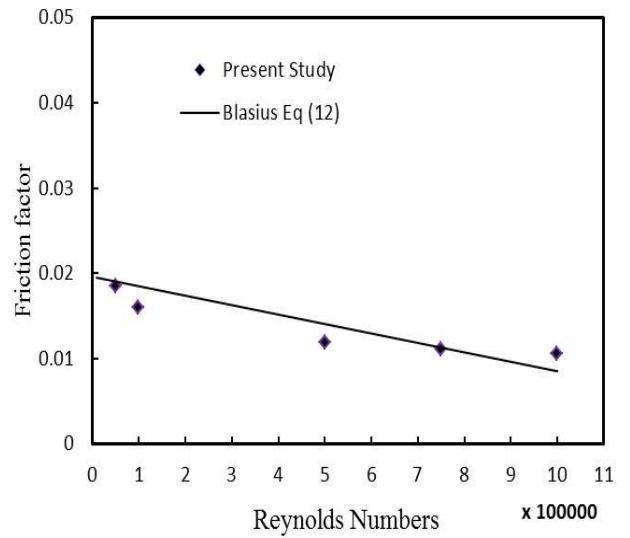
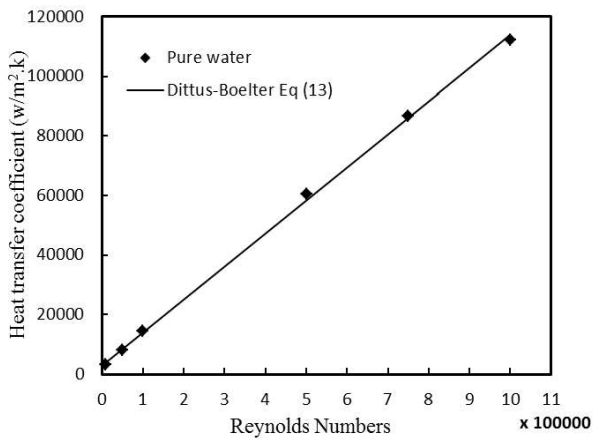


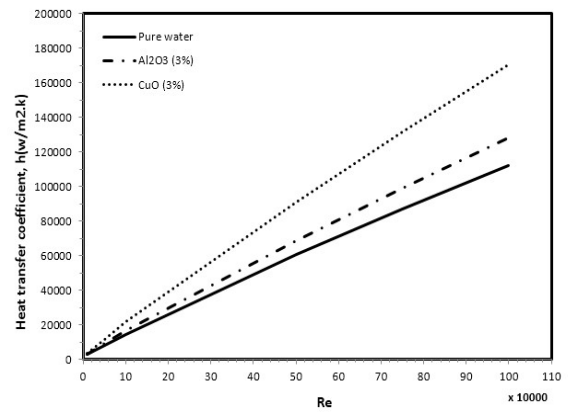
Fig. 2. Grid independent test



a. Friction factor

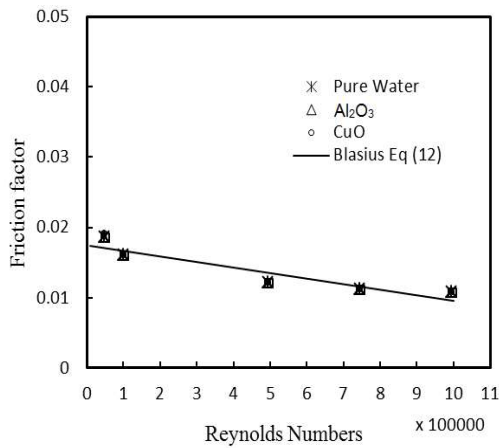


b. Heat transfer coefficient



b. Heat transfer coefficient

Fig. 4. Comparison of the computed values for pure water and nanofluids in turbulent regime.



a. Friction factor

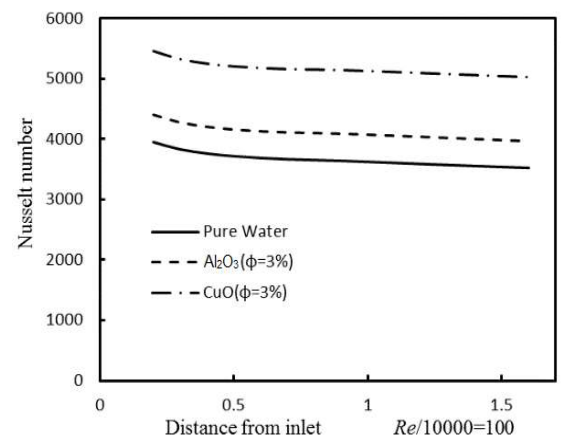


Fig. 5. Local Nusselt number with the length of tube

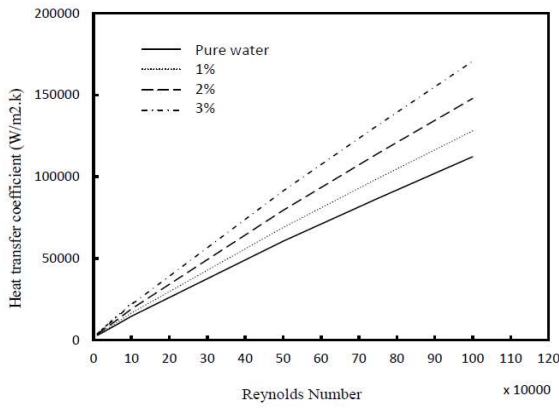


Fig. 6. The effect of nanofluid concentration on the heat transfer coefficient at Reynolds number

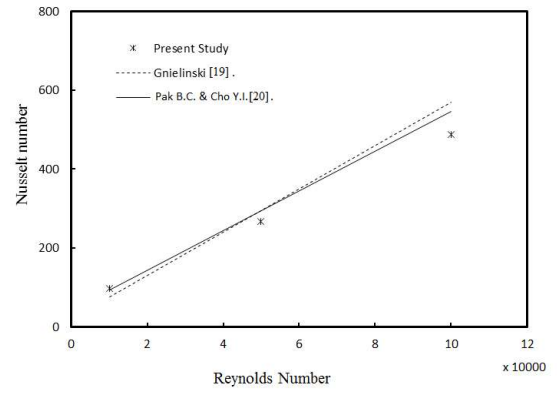


Fig. 7. Nusselt numbers validation.

Table 1. Physical properties of metal oxide nano materials

Type of fluid	$\phi$ (%)	$\rho$ (kg/m <sup>3</sup> )	$\mu$ (mpa.s)	$C_p$ (J/kg.k)	$K_{eff}(w/m.k)$	$pr$
Pure water	0	997.7	0.949	4178.9	0.6	6.6
CuO/water	1	1050.8	1.03	3960	0.616	6.61
CuO/water	2	1104	2.43	3762.1	0.632	14.4
CuO/water	3	1157.1	2.67	3582.4	0.65	14.7
Al <sub>2</sub> O <sub>3</sub> /water	1	1027.4	1.02	4046.96	0.617	6.7
Al <sub>2</sub> O <sub>3</sub> /water	2	1057.2	1.13	3922.46	0.635	7
Al <sub>2</sub> O <sub>3</sub> /water	3	1086.9	1.26	3804.78	0.653	7.3